

ANALYSIS OF COMBUSTION AND HEAT TRANSFER PERFORMANCE IN A SLIT-TYPE FULLY PREMIXED BURNER

by

Chen FANG^a, Lei SU^{a*}, Linghui CHEN^b, and Xuan JIANG^b

^aSchool of Energy Science and Engineering, Nanjing Tech University, Nanjing, China

^bZhejiang Guangtao Kitchen Co., LTD., Hangzhou, China

Original scientific paper

<https://doi.org/10.2298/TSCI240902253F>

Since most gas water heaters on the market still use diffusion or partially premixed combustion. Fully premixed combustion, with its advantages of complete combustion and low CO and NO_x emissions, offers a promising alternative. In response to this, a slit-type fully premixed gas water heater with a rated power of 20 kW was designed. The combustion and heat transfer performance, as well as the combustion temperature and burnout characteristics, were analyzed under ten different load conditions ranging from 100% to 8% using theoretical modelling. The study identified the variations in physical parameters and used numerical simulations to partially validate the theoretical results. Subsequently, by individually modifying structural variables, the optimal structure under single-variable conditions was determined. This optimal structure was then combined in various configurations to form a multi-variable structural design. Further theoretical analysis was conducted to assess whether the changes in the multi-variable structure, as well as the original design, met economic efficiency requirements. The results showed that the slit-type fully premixed burner achieved optimal performance when the number of burner plates was 120, with a length of 99 mm and a height of 10 mm.

Key words: full premixed combustion, gas water heater, theoretical analysis, numerical simulation

Introduction

In recent years, rapid urbanization has driven a substantial increase in energy consumption [1]. China heavily depend on imported energy, creating a growing shortage that can no longer meet rising demands. Consequently, energy conservation and emission reduction have become urgent global priorities. Gas water heaters, which are a primary source of hot water in households, now focus not only on meeting basic needs but also on enhancing safety, health, efficiency, and reducing emissions [2, 3]. The burner, being the most critical component of a gas water heater, plays a pivotal role in determining its efficiency and stability. Infrared gas burners have introduced a new direction in burner development [4], with metal radiant burners being one of the most notable advancements. Metal materials offer distinct advantages over other materials, including superior strength, rigidity, stability, and better resistance to thermal shock, brittleness, and thermal expansion. Significant progress has been made in combustion technology for gas water heaters, particularly in diffusion combustion, partially premixed combustion, and fully premixed combustion [5]. However, most gas water heaters on the market today still rely on partially premixed combustion. This presents a promising opportunity for the

* Corresponding author, e-mail: fangchen@njtech.edu.cn

application of fully premixed combustion in gas water heaters. This paper explores the combination of fully premixed combustion with metal fiber burners, providing a comprehensive theoretical analysis of the combustion and heat transfer mechanisms in slit-type fully premixed burners. It also investigates the burner's performance under varying load conditions, offering valuable insights for the study of combustion and heat transfer in fully premixed burners. Many researchers have contributed significantly to the study of fully premixed burners and gas water heaters. Liu [6] and colleagues conducted a detailed analysis of the heat transfer process and thermal characteristics of gas water heaters, using orthogonal experiments to examine how various parameters influence thermal efficiency. Their findings offered important guidance for gas water heater design. Huang [7] used numerical simulations and experimental validation investigate a new type of gas water heater. Their research highlighted the crucial role of the excess air ratio, showing that it affects not only combustion temperature and heat exchange efficiency but also emissions. Based on these results, they optimized the injector structure. A well-designed burner must not only achieve low pollutant emissions and high combustion efficiency but also maintain stable operating conditions, which is a key indicator of its quality. Xu, *et al.* [8] studied the flame stability of porous medium bluff bodies and found that fuel and air mixed more thoroughly behind the bluff body, broadening the flame stability range. Saracco, *et al.* [9] compared metal and ceramic burners, measuring CO emissions and temperature fields for both. They established a functional relationship between excess air ratio and surface heat intensity, exploring the operational characteristics of both burner types. Cerri, *et al.* [10] performed finite element modelling of metal mesh radiant burners, proposing an initial 1-D model to describe the combustion behavior inside porous burners. They also introduced models for energy, mass, and momentum balance within the burner, providing a quasi-homogeneous description of combustion. Cheng [11] designed a low swirl burner in which air was injected tangentially along the center jet of the premixed fuel upstream of the burner outlet, allowing the flame to burn across a wide range of equivalence ratios. Jensen and Shipman [12] developed flame-stabilizing ports that successfully stabilized high speed fully premixed flames while significantly reducing nitrogen oxide emissions.

Although there is substantial research on improving burner efficiency and reducing pollutant emissions, most studies focus on experiments based on low pressure, partially premixed burners, with limited systematic theoretical modelling of fully premixed burners under varying power levels. This paper aims to thoroughly analyze the combustion and heat transfer mechanisms of a gap-type fully premixed burner based on theoretical principles and investigate its performance under varying loads, providing a reference for theoretical analysis and research on the combustion and heat transfer processes of fully premixed burners.

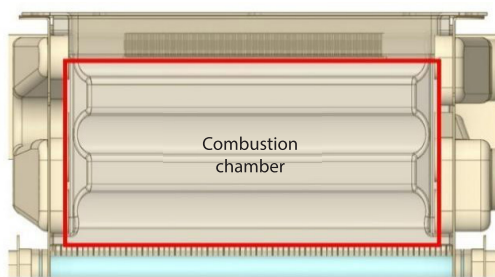


Figure 1. Side view of the combustion chamber 3- D structure

Structure of the slit-type fully premixed burner

The 3-D structural diagram and simplified schematic of the slit-type fully premixed burner are shown in figs. 1 and 2. The upper surface and side walls of the combustion chamber are lined with water-cooled walls, while the bottom is composed of 120 burner plates arranged in sequence. The thermal intensity requirements and structural parameters of the combustion chamber are detailed in tab. 1.

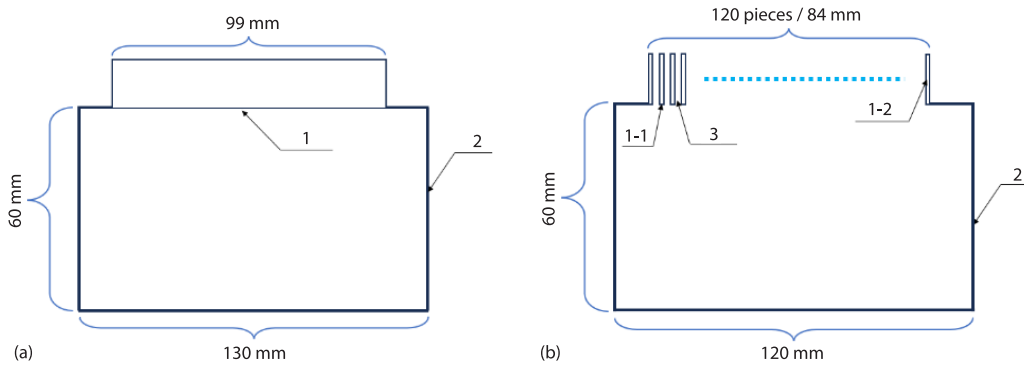


Figure 2. Simplified combustion chamber diagram: 1 – combustion strip.
 1-1 – burning sheet on the surface, 1-2 – side wall of combustion sheet,
 2 – combustion chamber; and 3 – seam between burning pieces

Table 1. Thermal intensity requirements

Name	Demand
Heat intensity of cavity section	780 mm ² per kW
Heat intensity of combustion section	415 mm ² per kW
Length	130 mm
Width	120 mm
Height	60 mm

Theoretical calculation process modelling

Given the complexity of the combustion and heat transfer processes in a slit-type fully premixed burner, this paper applies relevant theories to develop an internal combustion and heat transfer model for the burner [13]. The model incorporates the heat balance equation for the combustion chamber, the heat balance equation for the flame surface, a heat transfer model for the slits between the combustion plates, and a radiative heat transfer model for the combustion chamber, which includes the combustion plates and the cold side of the heat exchanger. By analyzing and coupling the heat transfer relationships within these models, iterative calculations are used to determine key parameters, such as the average flame temperature in the combustion chamber, the combustion plate temperature, the gas preheating temperature rise, and the radiative and convective heat transfer between different parts of the combustion chamber at rated power. Additionally, the model calculates the flame propagation speed, burnout characteristics, and residence time to assess whether the premixed flame experiences flashback or achieves complete combustion.

Working principle and model hypothesis

Before the premixed gas enters the combustion chamber, the fuel must be mixed with air to form a premixed gas. This premixed gas, influenced by a fully premixed injector, flows through the gaps between the burner plates into the combustion chamber, where it forms an inverted flat flame on the burner surface. The flame radiatively transfers heat to the burner plates, raising their temperature. These plates then preheat the premixed gas, facilitating its combustion, while also providing a stable heat source at the base of the flame, which helps maintain flame stability. For the theoretical model, the following assumptions are made: the calculated temperature

of the burner plates is uniform and the high temperature flat flame is in close contact with the exit of the gaps between the burner plates and has a certain height. Therefore, when calculating flame radiation, it is assumed that the flame radiates across the entire combustion chamber. Since the combustion products are mobile, the flame temperature is taken as the average temperature within the combustion chamber for theoretical calculations. The walls of the combustion chamber are fully covered with heat exchange pipes for heating circulating water, and the wall temperature has been determined based on subsequent heat exchanger requirements or standards. Thus, the wall temperature of the combustion chamber is assumed to be constant.

Heat of combustion of gas and heat balance of flame surface

The heat released from gas combustion is equal to the lower heating value of the gas multiplied by the gas flow rate:

$$Q_r = Q_{dw} q_v \quad (1)$$

where Q_r [kW] is the gas combustion gives off heat, Q_{dw} [MJN⁻¹m⁻³] – the low calorific value of gas, and q_v [Nm³s⁻¹] – the volume flow of gas.

Heat balance equation of flame surface

The radiant heat of the flame is equal to the radiant heat from the flame to the combustion plate, the radiant heat from the flame to the low temperature surface, and the enthalpy rise of the premixed gas from the preheated temperature to the flame temperature:

$$Q_r = Q_{f,h} = Q_{f,h,1} + Q_{f,h,2} + \Delta H_q \quad (2)$$

where $Q_{f,h}$ [kW] is the flame radiation heat, $Q_{f,h,1}$ [kW] – the flame faces the radiant heat of the burning sheet, $Q_{f,h,2}$ [kW] – the flame faces the radiating heat of the cryogenic surface, and ΔH_q [kW] – the enthalpy increase of premixed gas from preheated temperature to flame temperature.

The radiant heat transfer between the flame and the combustion plate is divided into two parts, one is the radiant heat transfer between the flame and the wall of the combustion plate, and the other is the radiant heat transfer between the flame and the side wall of the combustion plate:

$$Q_{f,h,1} = Q_{f,h,1-1} + Q_{f,h,1-2} \quad (3)$$

where $Q_{f,h,1-1}$ [kW] is the flame faces the radiant heat on the surface of the burning plate and $Q_{f,h,1-2}$ [kW] – the flame faces the radiant heat of the slit between the burning plates.

Radiation model of flame and burning surface

The radiation between the flame and the upper surface of the combustion plate can be viewed as a radiative heat transfer between the infinite plates:

$$Q_{f,h,1-1} = \frac{A_{1-1} \sigma (T_h^4 - T_{1-1}^4)}{\frac{1}{\varepsilon_h} + \frac{1}{\varepsilon_{1-1}} - 1} \quad (4)$$

$$\varepsilon_h = 1 - e^{-kP \frac{3.6V}{F}} \quad (5)$$

$$k = \left(\frac{7.8 + 16r_h}{3.16 \sqrt{\text{Pr} \frac{3.6V}{F}}} - 1 \right) \left(1 - \frac{0.37T_h}{1000} \right) r \quad (6)$$

where A_{1-1} [m²] is the total surface area of the burner, σ [Wm⁻²K⁻⁴] – the blackbody radiation constant, ($\sigma = 5.67 \cdot 10^{-8}$), T_h [K] – the mean flame temperature, T_{1-1} [K] – the burning sheet surface temperature, $\varepsilon_h, \varepsilon_{1-1}$ are the flame and burner emissivity, V [m³] – the combustion chamber volume, F [m²] – the combustion chamber surface area, k [MPa⁻¹m⁻¹] – the smoke attenuation factor, r, r_h are the volume share of three atomic gas and the volume share of water vapor, and P [Pa] – the pressure in the combustion chamber.

Model of slit radiation between flame and individual burning plate

The radiation model between the flame and the gap of a single combustion plate is shown in fig. 3. The h -surface represents the flame surface, the m -surface represents the sidewalls of the combustion plate, and the q -surface represents the inflow surface of the premixed gas. The distances ab and cd indicate the width of the gap, while ac and bd represent the height of the gap.

According to the algebraic analysis method, the angular coefficient $X_{h,m}$ of the h -surface relative to the q -surface is given:

$$X_{q,h} = \frac{(bc + ad) - (ac + bd)}{2cd} \quad (7)$$

$$X_{q,m} = 1 - X_{q,h} \quad (8)$$

The radiation heat transfer formula from the flame in a single gap to the sidewalls of the combustion plate is given:

$$Q_{f,h,1-2}^d = (E_{b,h} - E_{b,1-2}) A_h X_{h,m} \quad (9)$$

where $E_{b,h}, E_{b,1-2}$ [Wm⁻²] are the blackbody radiation intensities of the flame and the sidewalls within the gap of the combustion plate, A_h [m²] – the area of the sidewalls within the gap of the combustion plate, and $X_{h,m}$ – the angular coefficient of the flame relative to the sidewalls within the gap of the combustion plate.

The heat balance equation for the combustion plate and the interior of the gap

The radiant heat from the flame to the burner equals the sum of the radiant heat from the burner to the low temperature surface and the convective heat transfer of the premixed gas within the gap:

$$Q_{f,h,1} = Q_{f,1,2} + Q_d \quad (10)$$

where $Q_{f,1,2}$ [kW] is the radiant heat from the combustion plate and the gap to the low temperature surface and q_d [kW] – the convective heat transfer of the premixed gas within the gap.

Radiant heat transfer from the burner to the low temperature surface

The radiative heat transfer from the burner to the low temperature surface consists of two parts: radiation from the burner’s upper surface and radiation from the slits between the combustion plates. Due to the narrow width of the slits, they can be considered as black bodies. For ease of calculation, radiation from the slit sides is converted to radiation from the upper surfaces of the slits, and this is weighted with the radiation from the upper surface of the combustion plates to determine the overall emissivity of the burner’s upper surface.

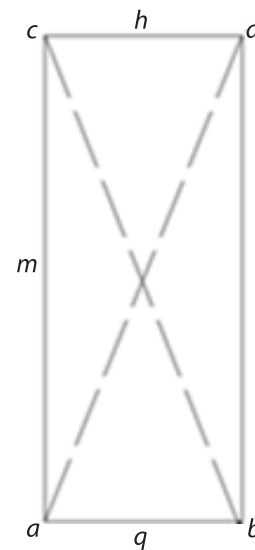


Figure 3. Radiation model of the flame and combustion plate sidewalls

The formula for the radiant heat from the burner to the low temperature surface $Q_{f,1,2}$:

$$Q_{f,1,2} = \frac{E_{b,1} - E_{b,2}}{\frac{1 - \varepsilon_1}{\varepsilon_1 A_1} + \frac{1}{A_1 X_{1,2}} + \frac{1 - \varepsilon_2}{\varepsilon_2 A_2}} \quad (11)$$

where $E_{b,1}$ and $E_{b,2}$ are the blackbody radiation intensities of the combustion plate and the low temperature surface, respectively, ε_1 and ε_2 – the effective emissivities of the combustion plate and the low temperature surface, respectively, A_1 and A_2 [m²] are the radiative areas of the burner and the low temperature surface, and $X_{1,2}$ is the angular coefficient of the combustion plate relative to the low temperature surface.

The equation for the weighted emissivity of the burner:

$$\varepsilon_1 = \frac{(P_1 D_1 \varepsilon_{1-1} - P_2 D_2) L}{A_1} \quad (12)$$

where P_1 and P_2 are the number of combustion plates and gaps, respectively, D_1 and D_2 [m] – the widths of the combustion plates and gaps, and L [m] – the length of the combustion plate.

Convective heat transfer of the premixed gas within the gap

The convective heat transfer process of the premixed gas within the gap can be modeled as fluid-flowing longitudinally through a multi-layer metal mesh. The empirical equation for convective heat transfer:

$$Q_d = h A_{1-2} \Delta T \quad (13)$$

$$\text{Nu} = 2.5 \cdot 10^{-2} \text{Re}^{0.97} \text{Pr}^{1/3} \quad (14)$$

$$h = \frac{\text{Nu} \lambda}{l} \quad (15)$$

where h [Wm⁻²K⁻¹] is the convective heat transfer coefficient, A_{1-2} [m²] – the convective heat transfer area of the gap sidewalls, ΔT [K] – the temperature difference for convective heat transfer, Re, Pr, and λ [Wm⁻¹K⁻¹] are the Reynolds number, Prandtl number, and thermal conductivity of the premixed gas at a given temperature, respectively, and l [m] – the characteristic dimensions.

Heat balance equation for the temperature rise of the premixed gas

Since the premixed gas undergoes a temperature rise through convective heat transfer within the slit, the convective heat transfer between the premixed gas and the combustion plate in the slit should equal the heat absorbed by the premixed gas:

$$Q_d = q_m (c_{p,q,d} T_d - c_{p,q,0} T_0) \quad (16)$$

where q_m [kgs⁻¹] is the mass-flow rate of the premixed gas, $c_{p,q,d}$, $c_{p,q,0}$ [Jkg⁻¹K⁻¹] are the specific heat capacity at constant pressure of the premixed gas at its preheated temperature and initial temperature, and T_d , T_0 [K] – the preheated temperature and initial temperature of the premixed gas.

Flame stability and burnout performance analysis model

Stable flame combustion is essential for a water heater system. During the combustion process, the combustion plates absorb radiant heat from the flame and reach high temperatures. This enables them to preheat the premixed gas before it enters the combustion chamber, promoting more complete combustion and providing additional heat to the flame's base. To

maintain stable 2-D flame combustion, the flow rate of the premixed gas must exceed the flame propagation speed.

For laminar premixed flame propagation speed, S_L , which is influenced by the temperature of the unburned premixed gas T_0 , it can be analyzed:

$$S_L = \sqrt{2 \left(\frac{\lambda}{c_{p,q,0} \rho_0} \right) \left(\frac{\bar{W}}{C_{f,0}} \right)} = \sqrt{\frac{2a}{\bar{\tau}}} \quad (17)$$

where λ [$\text{Wm}^{-1}\text{K}^{-1}$] is the thermal conductivity of the premixed gas, ρ_0 [kgm^{-3}] – the initial density of the premixed gas, \bar{W} [$\text{kmolm}^{-3}\text{s}^{-1}$] – the average combustion reaction rate, $C_{f,0}$ [molm^{-3}] – the concentration of the combustible gas in the unburned mixed gas, a [m^2s^{-1}] – the thermal diffusivity, and $\bar{\tau}$ [second] – the Burnout time of the combustible mixed gas.

Criteria and conclusion analysis

The four performance indicators are: average flame temperature, combustion plate temperature, preheat temperature (the temperature of the premixed gas after being preheated in the slit between the combustion plates), and the comparison between burnout time and residence time. Using a nominal power of 20 as a reference, this paper calculates the average flame temperature, combustion plate temperature, preheated premixed gas temperature, flow velocity within the slits, flame propagation speed, residence time of the premixed gas in the combustion chamber, and burnout time under ten different power levels, ranging from 100% to 8% load. Additionally, the ratio of burnout time to residence time is determined.

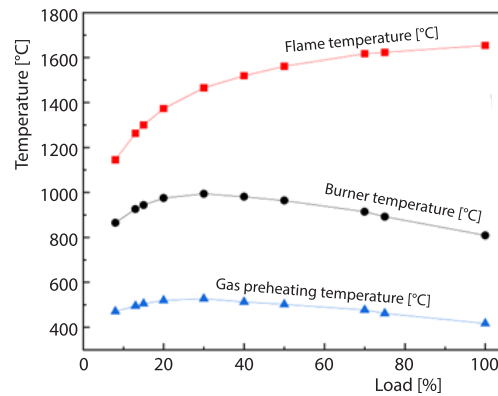


Figure 4. Variation of temperatures with load changes

Analysis of the theoretical calculations and results for the original structure

Comparison of temperature variations in the original structure under varying power levels

Figure 4 illustrates that as the combustion load increases from 8% to 100%, the average temperature in the combustion chamber (flame temperature) rises. This increase is due to the higher mass-flow rate of the premixed gas entering the chamber, which subsequently elevates the flame temperature. The preheating temperature of the combustion plate and the premixed gas initially increases before decreasing, reaching a maximum at 30% load. When the load exceeds 30%, even though it drops from 100% to 30%, the flame temperature in the combustion chamber does not decrease sharply. Instead, the primary change is the reduction in the volume flow rate of the premixed gas. This decrease results in a lower flow velocity through the

combustion plate gaps and a longer residence time, which weakens the convective heat transfer between the gap walls and the premixed gas. Consequently, the temperatures of the combustion plate and the premixed gas rise as the load decreases. When the load falls below 30%, decreasing from 30% to 8%, the overall combustion heat of the premixed gas diminishes, leading to lower flame temperatures, combustion plate temperatures, and preheating temperatures of the premixed gas. Therefore, the peak at 30% load can serve as a valuable reference for designing the combustion plate and assessing whether the premixed gas might ignite prematurely in the gaps of the combustion plate.

Comparison of flow rate and time variations in the original structure under varying power levels

Figure 5(a) shows that as the load decreases from 100% to 8%, the flow velocity of the premixed gas remains consistently above the flame propagation speed. This indicates that under the slit-type fully premixed burner structure discussed in this paper, flashback is not an issue, and the burner remains stable even at low loads. Figure 5(b) demonstrates that as the load decreases from 100% to 8%, the residence time of the premixed gas in the combustion chamber consistently exceeds the burnout time required for complete premixed combustion. This suggests that the burner maintains complete combustion across varying power levels with this structure.

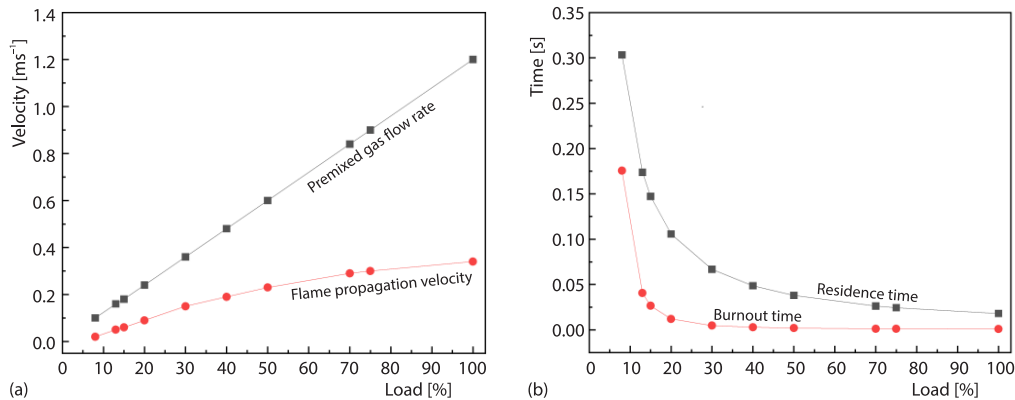


Figure 5. Comparison of flow rate and time; (a) flow rate comparison and (b) time comparison

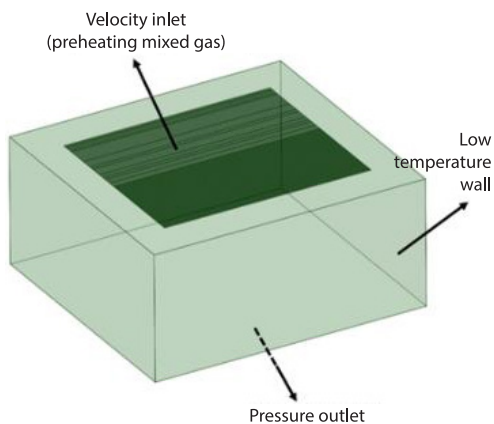


Figure 6. Physical model of the combustion chamber

Numerical simulation of combustion within the combustion chamber

Physical model

A physical model of the combustion chamber was established based on its structural dimensions, as shown in fig. 6.

Set-up of the computational model and boundary conditions

The standard $k-\varepsilon$ model has been proven through numerous engineering applications to be highly accurate, which is why this turbulence model was selected for the study. For simulating the premixed combustion of methane and

air inside the combustion chamber, which involves chemical reactions and energy conservation, the Eddy-Dissipation [14] model was chosen. To achieve better convergence results, the pressure-velocity coupling was solved using the Coupled algorithm [15, 16], which simultaneously resolves the pressure and velocity equations. The pressure term was discretized using the PRESTO scheme, while the other terms were handled with second-order upwind schemes. The specific boundary conditions are detailed in tab. 2.

Table 2. Boundary condition

Parameter	Value
The temperature of low temperature surface [°C]	357
The thermal emissivity of a low temperature surface	0.4
Premixed gas inlet	Velocity-inlet, flow rate is calculated by reference to the volume flow rate at the temperature after being preheated, and the temperature is the preheating temperature
Premixed gas outlet	Pressure outlet
Radiation model	P1

Mesh independence analysis

Unstructured mesh grids were created using FLUENT Meshing. To ensure mesh independence, simulations were performed for a 30% load with four different mesh densities ranging from 2 million 8 million cells. The mesh configurations and the average flame temperature results within the combustion chamber are shown in figs. 7 and 8. Ultimately, a mesh with 6 million cells was selected for multi-condition simulations.

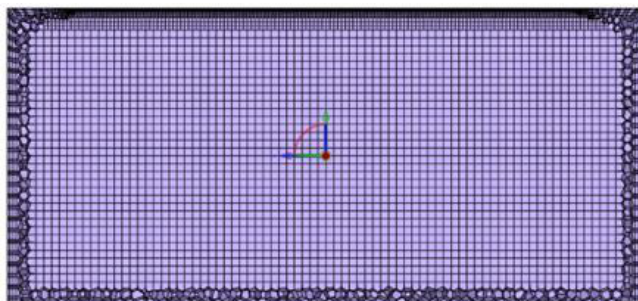


Figure 7. Mesh division

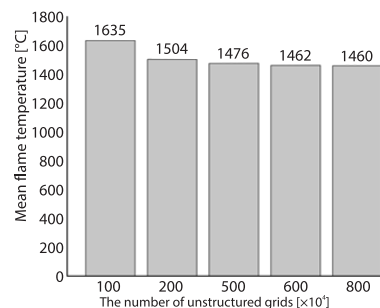


Figure 8. Mesh independence analysis

Results analysis

Comparison of theoretical and simulated results

Figure 9 shows the flow field distribution at the peak point of 30% combustion load as obtained from FLUENT simulations. Subsequently, the average flame temperature within the combustion chamber was calculated for loads ranging from 100% to 8%. An error analysis comparing these results with theoretical calculations is illustrated in fig. 10.

Figure 9 shows that the flame surface formed by the combustion of premixed gas in the combustion chamber is planar, consistent with the theoretical model’s assumption of a planar flame at the slit exit. This confirms the validity of the model’s assumptions. Figure 10 indicates that the average flame temperature within the combustion chamber, obtained from numerical simulations across ten different load conditions ranging from 100% to 8%, follows a

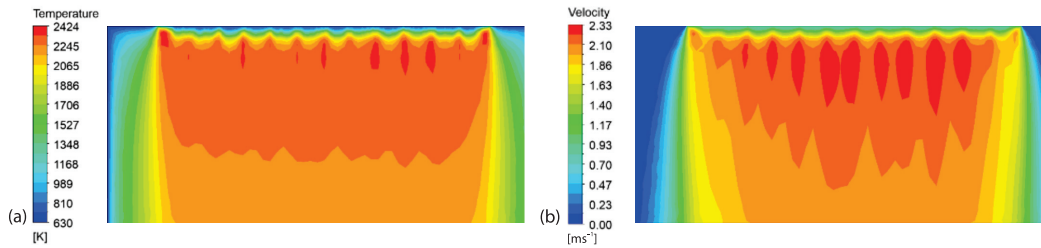


Figure 9. Flow field distribution within the combustion chamber; (a) temperature field distribution and (b) velocity field distribution

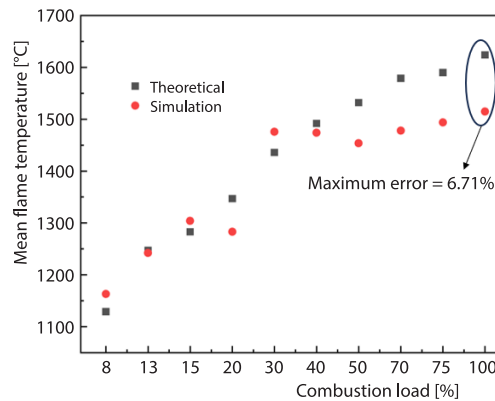


Figure 10. Comparison of theoretical and simulated average flame temperatures under varying loads

trend similar to that predicted by the theoretical model, with a maximum error of only 6.71%, well within acceptable engineering error limits. This demonstrates the accuracy of the proposed theoretical model and assumptions, providing a reliable foundation for future studies exploring different structural variations.

Impact of structural variations on combustion and heat transfer performance

The study investigates how changes in individual variables – such as the number of combustion plates, plate length, and plate height – affect flame temperature, plate temperature, and preheat temperature. By analyzing these variables, the optimal structure for each single-variable scenario is determined.

Performance analysis with varying number of combustion plates

Figures 11(a)-11(c) show that when only the number of combustion plates is altered, the trends in flame temperature, combustion plate temperature, and gas preheating temperature remain consistent with the original structure. However, changes in the number of plates result in variations in temperature values, which in turn affect the modified structure. As the number of combustion plates increases, the flame temperature decreases, with each increment of five plates causing a reduction of 7° C to 3 °C. This decrease is more pronounced at lower loads, and a minimum flame temperature above 1110 °C is beneficial for the complete combustion of the premixed gas. When the plate count increases and the load exceeds 30%, both the combustion plate temperature and preheating temperature decrease. However, when the load falls below 30%, these temperatures rise, with the highest preheating temperature reaching 527 °C, which is still below the ignition temperature of the premixed gas (632 °C). Burnout

time is influenced by combustion under varying operational conditions. This study uses the ratio of burnout time to residence time under 100%, 30%, and 8% load as a reference, with a particular focus on assessing combustion efficiency at low loads – one of our primary concerns. Figure 11(d) reveals that combustion is efficient at loads between 30% and 100%. However, when the load drops below 30%, some single-variable structures show burnout times approaching 90% of the residence time, theoretically indicating a risk of incomplete combustion if the system becomes even slightly unstable. Finally, through comparative analysis, we found that the optimal performance in terms of temperature and time ratios is achieved when the number of combustion plates is between 120 and 125.

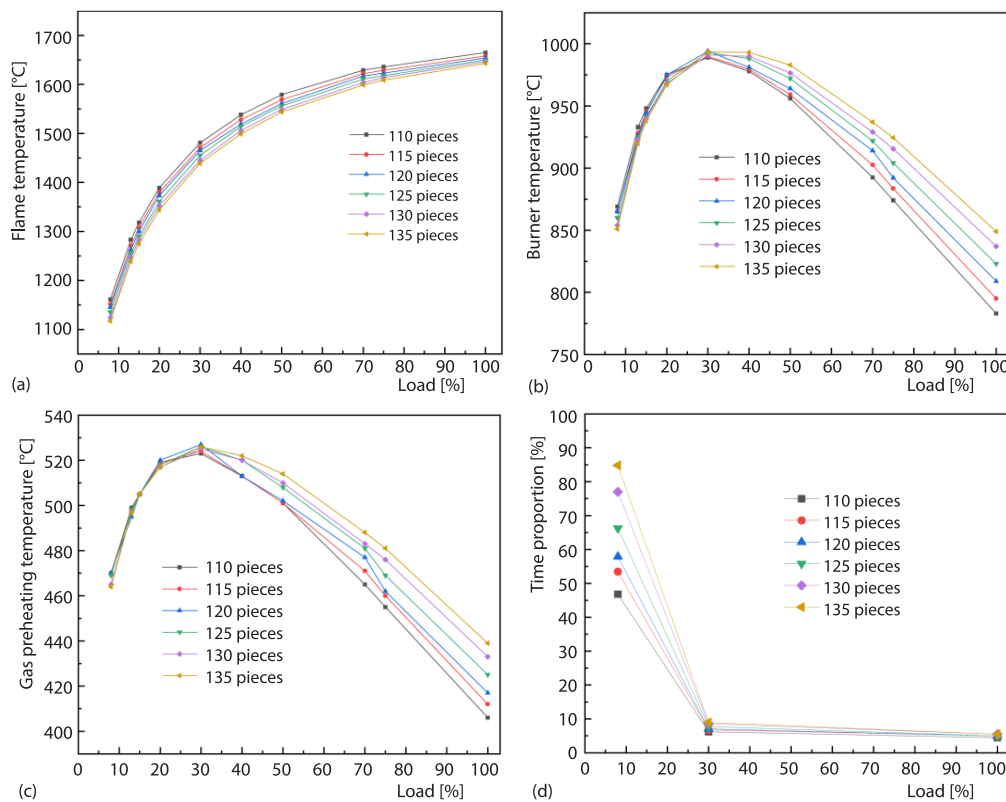


Figure 11. Performance analysis with varying number of combustion plates;
 (a) flame temperature, (b) combustion plate temperature, (c) gas preheat temperature, and
 (d) ratio of burnout time to residence time

Performance analysis with varying combustion plate length

Figure 12(a)-12(c) show that as the length of the combustion plates increases, the flame temperature decreases, dropping by about 3 °C for every 3 mm added. This decline becomes more pronounced at lower loads, although the minimum flame temperature still exceeds 1110 °C. As the length of the combustion plates increases, at loads above 30%, both the combustion plate temperature and preheating temperature decrease. However, below 30% load, these temperatures begin to rise. Figure 12(d) shows that combustion is sufficient when the load is between 30% and 100%. However, when the load drops below 30%, in certain single-variable configurations, the burnout time approaches 70% of the residence time, increasing the

likelihood of incomplete combustion. Overall, combustion plates with lengths of 96 mm and 99 mm demonstrate moderate temperatures with relatively stable fluctuations. Comparative analysis reveals that, at low loads, the ratio of burnout time to residence time is also moderate for plates of these lengths, indicating a more balanced performance.

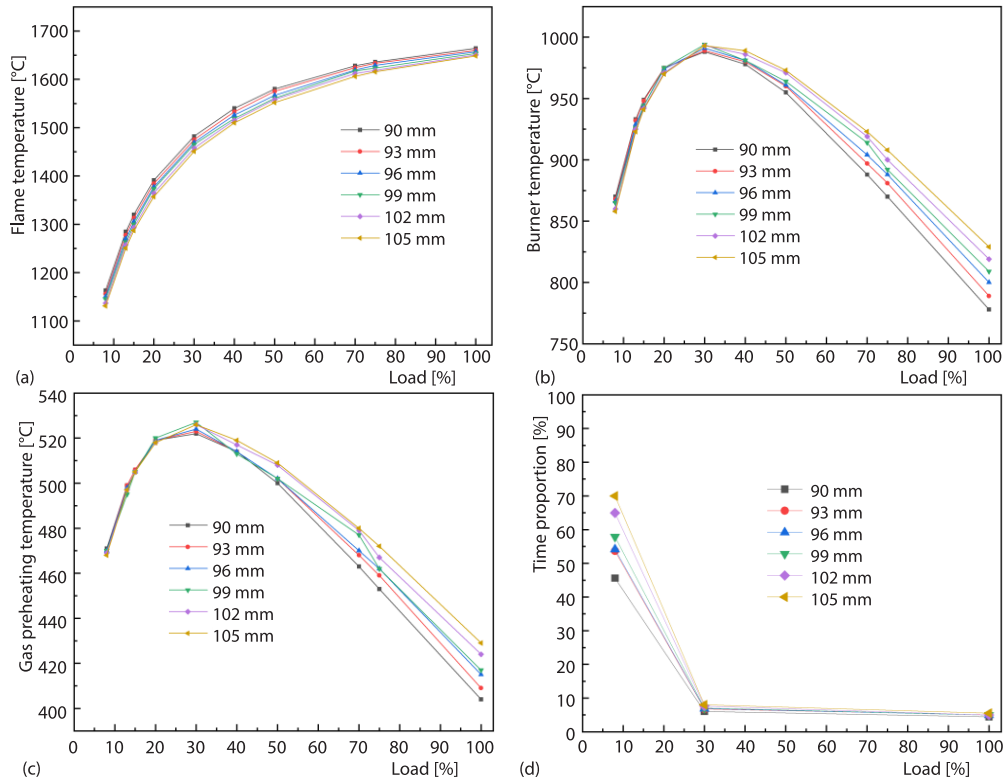


Figure 12. Performance analysis with varying combustion plate length; (a) flame temperature, (b) combustion plate temperature, (c) gas preheat temperature, and (d) ratio of burnout time to residence time

Performance analysis with varying combustion plate height

Figures 13(a)-13(c) show that as the height of the combustion plates increases, the flame temperature shows a slight upward trend. At the same height, the lower the load, the more significant the temperature decrease, although the minimum flame temperature still exceeds 1110 °C. As the combustion plate height increases, the combustion plate temperature tends to decrease, likely due to the increased surface area for convective heat transfer between the premixed gas and the combustion plates. At the same combustion plate height, the plate temperature decreases when the load is above 30%, but rises when the load is below 30%. The increase in combustion plate height also enhances the convective heat transfer area between the premixed gas and the combustion plates, strengthening the gas preheating process, which raises the gas preheating temperature. At the same plate height, the preheating temperature decreases when the load is above 30%, but rises below 30%. Comparatively, when the plate height reaches 11 mm, the preheating gas temperature exceeds the ignition temperature, potentially causing combustion within the gaps between the plates, which could shorten the lifespan of the combustion plates. Figure 13(d) shows that combustion is sufficient at loads between 30% and

100%. However, when the load drops below 30%, the maximum burnout time accounts for 50% of the residence time, which is an improvement over the previous two structural changes. Nevertheless, the potential for incomplete combustion remains at low loads. Through comparative analysis, we found that a combustion plate height of 10 mm offers the best overall performance.

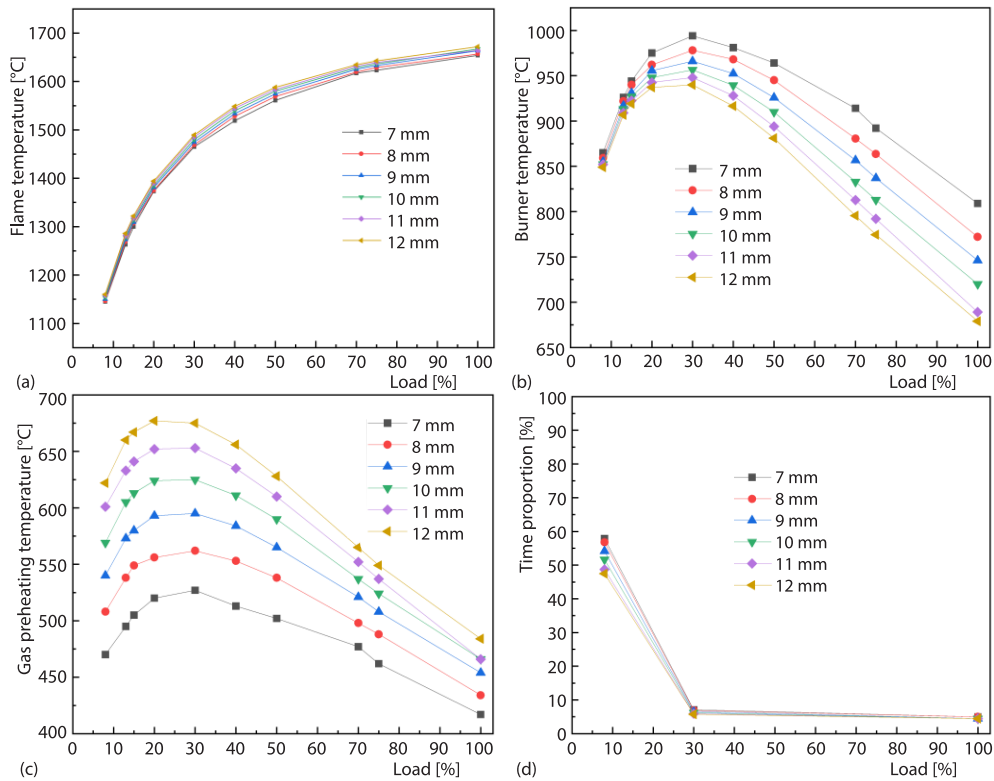


Figure 13. Performance analysis with varying combustion plate height; (a) flame temperature, (b) combustion plate temperature, (c) gas preheat temperature, and (d) ratio of burnout time to residence time

Conclusions from single-factor variable analysis

The optimal structural dimensions derived from the single-factor variable analysis are shown in tab. 3.

Table 3. Optimal structural combinations

Optimal number of combustion plates	Optimal combustion plate length [mm]	Optimal combustion plate height [mm]
120	96	10
125	99	

Performance comparison under multi-factor integration

The analysis results under a single variable were combined into four combinations, which were then compared. Among these, only Type 1 (120 burner plates, 99 mm in length, and 10 mm in height) and Type 2 (125 burner plates, 96 mm in length, and 10 mm in height)

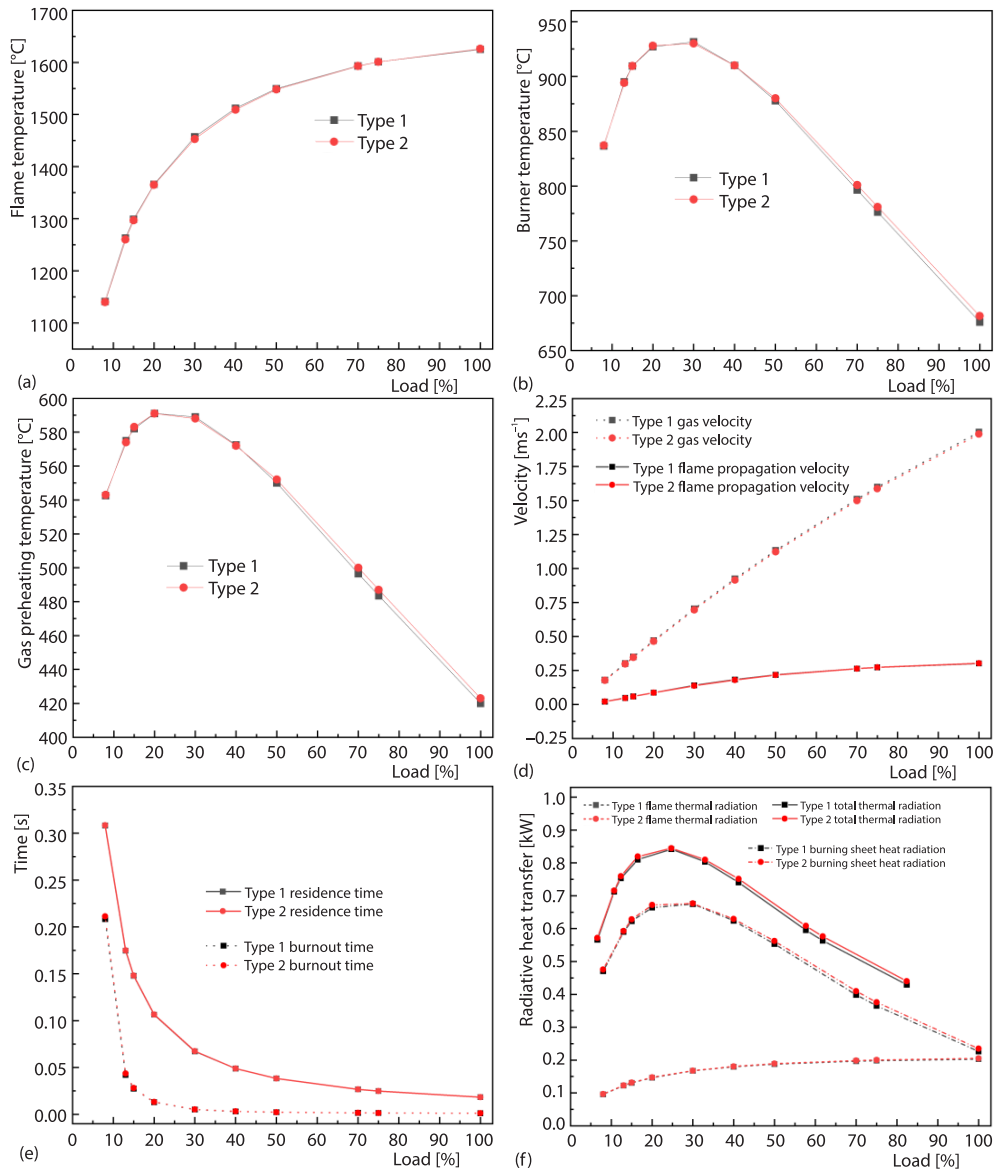


Figure 14. Performance comparison under multi-factor integration;
(a) flame temperature, (b) combustion plate temperature, (c) gas preheat temperature,
(d) comparison of gap flow rate and flame propagation speed,
(e) comparison of residence time and burnout time, and (f) comparison of radiant heat quantities

were found to be optimal. Further comparisons of flame temperature, burner plate temperature, preheating temperature, interstitial flow velocity, flame propagation speed, residence time, and burnout time revealed consistent trends and similar values for both structures as shown in fig. 14. Considering various factors, Type 1 emerges as the best choice for several reasons. Firstly, the longer burner plate length in Type 1 allows for greater diffusion of the premixed gas within the combustion chamber, reducing the size of the vortices formed at the sidewalls and ensuring more

uniform heating of the low-temperature surface. Secondly, from an economic perspective, the modification to Type 1 involves only a slight increase in plate height to 10 mm, requiring minimal changes to the original model and facilitating later processing due to fewer plates compared to Type 2. In summary, Type 1 is the optimal choice based on these considerations.

Conclusions

The following conclusions are drawn from the analysis.

- The flame temperature consistently decreases as the load drops from 100% to 8%. The temperatures of the combustion plates and the preheat temperature initially increase and then decrease, with a peak occurring at approximately 30% load.
- Under single-factor structural parameter variations, the optimal number of combustion plates is 120 or 125, the optimal combustion plate length is 96 mm or 99 mm, and the optimal combustion plate height is 10 mm.
- By combining the optimal structural configurations for single-variable parameters and considering the economic feasibility of modifications to the original structure, the best configuration for the gap-type fully premixed burner is determined to be 120 combustion plates, a combustion plate length of 99 mm, and a combustion plate height of 10 mm.

Nomenclature

A_1 – radiative area of the burner	Re – Reynolds number
A_2 – low temperature surface area	T_h – average flame temperature
$A_{1,1}$ – total surface area of the burner	ΔT – convective heat transfer temperature difference
a – thermal diffusivity	$X_{1,2}$ – angle coefficient of the folded combustion sheet to the low temperature surface
C_{t0} – concentration of combustible gas in the unburned gas mixture	V – combustion chamber volume
E_b – blackbody radiant force	
F – combustion chamber surface area	<i>Greek symbols</i>
h – convective heat transfer coefficient	λ – thermal conductivity of premixed gas
l – qualitative dimensions	σ – blackbody radiation constant
P – pressure	
Pr – Prandtl number	

References

- [1] Fu, Z., C., *et al.*, *New Technology of Natural Gas Combustion and Energy Saving and Environmental Protection*, Architecture and Construction Press, Beijing, China, 2007
- [2] Zhuang, Y. M., *Combustion and Pollutant Control*, Tongji University Press, Shanghai, China, 1995
- [3] Peng, *Design and Experimental Study of a Fully Blown-Type Partially Premixed Burner for Gas Water Heaters*, Chongqing University, Chongqing, China, 2017
- [4] Bao, T., *Numerical Simulation and Experimental Study on Combustion Characteristics of Ultra-Low Nitrogen Metal Fiber Burner*, Nanjing University of Science and Technology, Nanjing, China, 2018
- [5] ***, *Gas Combustion and Application*, China Building and Construction Press, Tongji University, Shanghai, China, 2011
- [6] Liu, M. L., *Study on Thermal Characteristics of Forced Exhaust Gas Water Heater*, Chongqing University, Chongqing, China, 2005
- [7] Huang., *Numerical Simulation and Experimental Study of the Combustion Process in a New Type of Gas Instant Water Heater*, Chongqing University, Chongqing, China, 2006
- [8] Xu, S., *et al.*, Experimental Study on Flame Stability Characteristics of Porous Medium with Blunt Body, *Journal of University of Science and Technology of China*, 41 (2011), 5, 445
- [9] Saracco, G., *et al.* On the Potential of Fibre Burners to Domestic Burners Applications – An Experimental Study, *Gas Waerme International*, 45 (1996), 1, pp. 24-31
- [10] Cerri, I., *et al.*, Improved-Performance Knitted Fibre Mats as Supports for Pre-Mixed Natural Gas Catalytic Combustion, *Chemical Engineering Journal*, 82 (2001), 1-3, pp. 73-85

- [11] Cheng, R. K., Velocity and Scalar Characteristics of Premixed Turbulent Flames Stabilized by Weak Swirl, *Combustion and Flame*, 101 (1995), 1-2, pp. 1-14
- [12] Jensen, W. P., Shipman, C. W., Stabilization of Flame in High Speed Flow by Pilot Flames, in: *Symposium (International) on Combustion*, Elsevier, Amsterdam, The Netherlands, 1958, Vol. 7, No. 1
- [13] Zheng, D. M., *et al.*, Study on Heat Transfer Characteristics and Performance of the Full Premixed Cauldron Stove with Porous Media, *Energies*, 15 (2022), 24, 9523
- [14] Ma, L., *et al.*, Characteristics of Coal Powder Coupled with Ammonia Combustion and NO Formation under Deep Air Staging, *Clean Coal Technology*, 28 (2022), 3, pp. 201-213
- [15] Zhou, D., *Research on Fire Scene Computation and Simulation Based on Virtual Reality Platform*, University of Science and Technology of China, Anhui, China, 2009
- [16] Ma, S., *et al.*, Structure Design and Performance Optimization of Diverging Micro-Channel Heat Exchanger, *Chinese Journal of Engineering Thermophysics*, 44 (2023), 5, pp. 1296-1303